of about 3.4. The preconditioned conjugate gradient squared method appears to be a viable tool for improving the performance of panel codes.

References

[1]Johnson, F. T., "A General Panel Method for the Analysis and Design of Arbitrary Configurations in Incompressible Flows," NASA CR 3079, May 1980.

[2]Sonnenveld, P., "CGS, a Fast Lanczos-Type Solver for Nonsymmetric Linear Systems," *SIAM Journal of Scientific and Statistical Computing*, Vol. 10, No. 1, 1989, pp. 36–52.

[3]Sudhakar, K., Koruthu, S. P., and Shevare, G. R., "3D Wing Analysis Using a Low Order Panel Method," *Journal of the Aeronautical Society of India*, Vol. 38, No. 4, 1986, pp. 303–306.

[4]Fletcher, R., "Conjugate Gradient Methods for Indefinite Systems," *Lecture Notes in Mathematics*, Vol. 506, Springer–Verlag, Berlin, 1976, pp. 73–89.

[5]Saad, Y., "The Lanczos Biorthogonalization Algorithm and Other Oblique Projection Methods for Solving Large Unsymmetric Systems," *SIAM Journal of Numerical Analysis*, Vol. 19, No. 3, 1982, pp. 485–506.

[6]Vitaletti, M., "Solver for Unfactored Implicit Schemes," *AIAA Journal*, Vol. 29, No. 6, 1991, pp. 1003–1005.

[7]Boersen, S. J., and Elsenaar, A., "Tests on the AFWAL 65° Delta Wing at NLR: A Study of Vortex Flow Development Between Mach = 0.4 and 4," *Proceedings of the Symposium on International Vortex Flow Experiment on Euler Code Validation* (Stockholm, Sweden), FFA, Bromma, Sweden, 1986, pp. 23–36.

Correct Limit Approximations for Planar, Cylindrical, and Spherical Blast Waves

Qifeng Zhu,* Wataru Masuda,† and Kiyoshi Yatsui‡
Nagaoka University of Technology, Nagaoka, Niigata 940-21, Japan

Introduction

THE blast wave refers to the shock-bounded flowfield produced by an energy release along a plane, a line, or at a point, which is called planar, cylindrical, and spherical blast wave, respectively. The energy is assumed to be infinitely concentrated and released instantaneously. Viscosity, thermal conductivity, real gas effects, and radiant energy losses in the flowfield behind the shock front are neglected. The flowfield ahead of the shock front is assumed to be uniform. The idealized problem of a strong explosion represents a typical example of a self-similar flow. The similarity solutions were found by Taylor[1] in connection with atomic bomb research. The first-order theory of a strong cylindrical blast wave was given by Sakurai[2] and Lin.[3] For a strong blast wave, the initial gas pressure is very small in comparison with the pressure behind the shock wave and can be neglected. This is equivalent to neglecting the initial internal energy of the gas in comparison with the explosion energy. When the shock wave becomes so weak that the initial pressure is no longer negligible compared with the pressure behind the shock, the first-order theory will be incorrect. This occurs near Mach number of 3.3 when the pressure ratio across the shock front drops below 10. The second-order theory, which gives a correction to the first-order theory for intermediate and weak waves, has been proposed by Sakurai.[4] As shown by Vlases and Jones,[5] the first-order theory fits the experimental points very well only for strong waves. However, Sakurai's second-order approximation appears to give too large a correction to the first-order theory for intermediate and weak waves. The correction term in a power series expansion in M^{-2n} (M is shock Mach number, $n = 1, 2, \ldots$) in Sakurai's high-order theory is slowly convergent. Based on the snowplow theory, Vlases and Jones have obtained a correct limit approximation for a cylindrical wave that predicts the shock trajectory very well down to $M = 1.16$.

It is the purpose of this paper to propose a simple method and develop the correct limit formulas to predict the shock trajectories over a wide range for planar, cylindrical, and spherical blast waves.

Brief Review of High-Order Theory and Snowplow Theory

Sakurai's High-Order Theory

Sakurai has obtained the solution in the form

$$(1/M^2)(\bar{R}_0/R)^{\alpha+1} = J_0[1+\lambda_1(1/M)^2+(\lambda_2/2)(1/M)^4+\cdots] \quad (1)$$

where R and $\bar{R}_0$ are the distance of shock front from the charge and the characteristic radius, respectively. Furthermore, $\alpha = 0$, 1, and 2 corresponds to a planar, a cylindrical, and a spherical wave, respectively, and J_0 and $\lambda_i (i = 1, 2, \ldots)$ are the constants. The values of J_0 and λ_1 have been given in Refs. 2 and 4. For example, $J_0 = 0.877$ and $\lambda_1 = -1.989$ for $\alpha = 1$ and $\gamma = 1.4$.

Sakurai has defined $\bar{R}_0$ as $(\bar{E}_\alpha/p_0)^{1/(\alpha+1)}$, where $\bar{E}_\alpha = \int_0^R [\rho u^2/2 + (p - p_0)/(\gamma - 1)]r^\alpha \, dr$, and u, p, and ρ are the flow velocity, the pressure, and the density, respectively. In addition, p_0, γ, and r are the pressure of undisturbed fluid, the ratio of specific heats, and the coordinate, respectively. In this paper, however, we alternatively define R_0 as $R_0 = (4E_\alpha/B\gamma p_0)^{1/(\alpha+1)}$, where for $\alpha = 0$, 1, or 2; $E_\alpha = \bar{E}_\alpha$, $2\pi\bar{E}_\alpha$, or $4\pi\bar{E}_\alpha$; and $B = J_0/\gamma$, $2\pi J_0/\gamma$, or $4\pi J_0/\gamma$, respectively. Therefore, we have $R_0 = (4\bar{E}_\alpha/p_0 J_0)^{1/(\alpha+1)} = (4/J_0)^{1/(\alpha+1)}\bar{R}_0$. Then Eq. (1) becomes

$$(1/M^2)(R_0/R)^{\alpha+1} = 4\left[1+\lambda_1(1/M)^2+(\lambda_2/2)(1/M)^4+\cdots\right] \quad (2)$$

The first-order and second-order approximations are given by Eqs. (3) and (4), respectively, as

$$(1/M^2)(R_0/R)^{\alpha+1} = 4 \quad (3)$$

$$(1/M^2)(R_0/R)^{\alpha+1} = 4\left[1 + \lambda_1(1/M)^2\right] \quad (4)$$

Integrating Eq. (4), we can obtain the following shock trajectory equation for $\gamma = 1.4$ and $\alpha = 1$:

$$\tau = 0.251\left[(1 + 7.96\lambda^2)^{\frac{1}{2}} - 1\right] \quad (5)$$

where λ and τ are defined as $\lambda = R/R_0$ and $\tau = Ct/R_0$, and C and t are the sound velocity of undisturbed fluid and the time, respectively.

Snowplow Theory

The similarity solution shows that almost all of the mass is contained within a thin layer near the front surface. In the snowplow model of Vlases and Jones, all of the mass is assumed to be concentrated in a thin layer at the shock front and travel with the shock velocity. By using this model, Vlases and Jones have obtained a simple expression for a cylindrical blast wave in the form

$$\tau = \tfrac{1}{2}\left[(1 + 4\lambda^2)^{\frac{1}{2}} - 1\right] \quad (6)$$

Correct Limit Conditions

The correct limit condition as $\lambda \to 0$ used in Ref. 5 for a cylindrical blast wave is

$$\tau = \lambda^2 \quad (7)$$

Here, we present a general expression as the correct limit condition for $\lambda \to 0$ based on Sakurai's first-order theory, since the agreement between the theory and experiment is very good for a strong wave. Substituting $M = d\lambda/d\tau$ and $\lambda = R/R_0$ into Eq. (3) and integrating, we have

$$\tau = 4(\alpha + 3)^{-1}\lambda^{(\alpha+3)/2} \quad (8)$$

Received Nov. 26, 1994; revision received June 20, 1995; accepted for publication July 5, 1995.

*Ph.D. Student, Department of Energy and Environment Science.
†Professor, Department of Mechanical Engineering.
‡Professor, Department of Electrical Engineering and Laboratory of Beam Technology.

which is the correct limit condition for $\lambda \to 0$. Equation (7) can be readily obtained from Eq. (8) if we substitute $\alpha = 1$.

The correct limit condition for $\lambda \to \infty$ is given by

$$M = \frac{d\lambda}{d\tau} = 1 \tag{9}$$

since the shock wave approaches the acoustic limit as $\lambda \to \infty$.

Description of Our Method

At first, we briefly review the technique employed by Vlases and Jones in obtaining their formula and, then, develop a simple method to predict the shock trajectories for planar, cylindrical, and spherical blast waves.

In the snowplow model of Vlases and Jones the total excess energy in the flowfield produced by a cylindrical blast wave, which must equal to the energy released in the explosion (E_α), is

$$\rho_0 \pi R^2 \left[F(\gamma)\dot{R}^2 - e_0\right] = E_\alpha \tag{10}$$

where $e_0 = (\gamma - 1)^{-1}(p_0/\rho_0)$, $F(\gamma) = \frac{1}{2} + 2(\gamma + 1)^{-2}$, and ρ_0 and e_0 are the density and the internal energy per unit mass of undisturbed fluid, respectively. One can integrate Eq. (10) to find that

$$\begin{aligned}\tau &= [2(\gamma - 1)F(\gamma)]^{\frac{1}{2}}[B\gamma(\gamma - 1)/4\pi]^{\frac{1}{2}} \\ &\quad \times \left(\{1 + [4\pi/B\gamma(\gamma - 1)]\lambda^2\}^{\frac{1}{2}} - 1\right) \\ &= \beta_1 \beta_2^{-\frac{1}{2}}\left[\left(1 + \beta_2\lambda^2\right)^{\frac{1}{2}} - 1\right]\end{aligned} \tag{11}$$

where $\beta_1 = [2(\gamma - 1)F(\gamma)]^{1/2}$ and $\beta_2 = 4\pi/B\gamma(\gamma - 1)$. For $\gamma = 1.4$, we have $B = 3.94$, $\beta_1 = 0.823$, $\beta_2 = 5.695$, and $F(\gamma) = 0.847$. Therefore, Eq. (11) becomes

$$\tau = 0.345\left[(1 + 5.695\lambda^2)^{\frac{1}{2}} - 1\right] \tag{12}$$

which has exactly the same form as Sakurai's second-order approximation of Eq. (5) except the constants. However, Eq. (12) does not satisfy the correct limit conditions of Eqs. (7) and (9). To satisfy the correct limit conditions, Vlases and Jones have chosen $\beta_1 = 1$ and $\beta_2 = 4$ and obtained Eq. (6).

We find in this study that the formula of Vlases and Jones for Eq. (6) can be readily obtained from Sakurai's second-order approximation of Eq. (4) if $\lambda_1 = -1$ and $\alpha = 1$. Now let us make an analysis of Sakurai's second-order approximation as $\lambda \to 0$ and $\lambda \to \infty$. From Eq. (4) for $\alpha = 1$ and noting that $M \to \infty$ as $\lambda \to 0$ ($R \to 0$), we have $(1/M^2)(R_0/R)^2 = 4$. After integrating, we have $\tau = \lambda^2$, which is the correct limit condition for $\lambda \to 0$ as mentioned before. That is to say that Sakurai's second-order approximation satisfies the correct limit condition for $\lambda \to 0$. As $\lambda \to \infty$ ($R \to \infty$), we find from Eq. (4) that $M = \sqrt{-\lambda_1}$. It is obvious that λ_1 given by Sakurai (-1.989 in this case) cannot satisfy Eq. (9), which is the correct limit condition for $\lambda \to \infty$. Therefore, we should choose a new value for λ_1 to satisfy the correct limit condition for $\lambda \to \infty$, which requires that $\lambda_1 = -1$.

Since Sakurai's second-order approximation has exactly the same form as the expression of Vlases and Jones obtained from the snowplow theory and satisfies the correct limit conditions if $\lambda_1 = -1$, it is clear that the expression of Vlases and Jones can be readily obtained from Sakurai's second-order approximation by letting $\lambda_1 = -1$. Substituting $\lambda_1 = -1$ and $\alpha = 1$ in Eq. (4), we have

$$M = \sqrt{1 + 4\lambda^2}/2\lambda \tag{13}$$

$$\tau = \int_0^\lambda \frac{2z}{\sqrt{1 + 4z^2}}\,dz = \frac{1}{2}\left[(1 + 4\lambda^2)^{\frac{1}{2}} - 1\right] \tag{14}$$

which is exactly the same as Eq. (6) given by Vlases and Jones.

Next, we will show that the preceding analysis also works well for a planar wave and a spherical wave. Generally, we have

$$\rho_0 \phi_\alpha R^{\alpha+1}\left[F(\gamma)\dot{R}^2 - e_0\right] = E_\alpha \tag{15}$$

where $\phi_\alpha = 1, \pi$, and $4\pi/3$ for $\alpha = 0, 1$, and 2, respectively. Equation (15) can be written in a different form as

$$(1/M^2)(\hat{R}_0/R)^{\alpha+1} = 4[1 + b(1/M)^2] \tag{16}$$

where $\hat{R}_0 = [4E_\alpha/\gamma F(\gamma)\phi_\alpha p_0]^{1/(\alpha+1)}$ and $b = -[\gamma(\gamma - 1)F(\gamma)]^{-1}$. We find that Eq. (16) has exactly the same form as Eq. (4) except the constants. The constants $\hat{R}_0$ and b in Eq. (16) should be chosen to satisfy the correct limit conditions. From Eq. (16), we have

$$(1/M^2)(\hat{R}_0/R)^{\alpha+1} = 4 \tag{17}$$

and $M = \sqrt{-b}$, for $\lambda \to 0$ and $\lambda \to \infty$, respectively. Substituting $M = d\lambda/d\tau$ and $R = \lambda R_0$ into Eq. (17) and integrating, we have $\tau = 4(\alpha + 3)^{-1}(R_0/\hat{R}_0)^{(\alpha+1)/2}\lambda^{(\alpha+3)/2}$. Comparing this expression with Eq. (8), we find that the correct limit condition for $\lambda \to 0$ will be satisfied if and only if $\hat{R}_0 = R_0$. Furthermore, b should be chosen to satisfy the correct limit condition for $\lambda \to \infty$, which requires that $b = -1$. Then Eq. (16) becomes $1/(M^2\lambda^{\alpha+1}) = 4[1 - (1/M)^2]$. After integrating, we can obtain the following formula to predict the shock trajectory:

$$\tau = \int_0^\lambda \sqrt{\frac{4z^{\alpha+1}}{1 + 4z^{\alpha+1}}}\,dz \tag{18}$$

From the preceding analysis, we see that the correct limit formulas can be readily obtained from Sakurai's second-order approximations if λ_1 is chosen as -1, without the complicated derivation as Vlases and Jones did.

Results and Discussion

Based on Eq. (18), we obtain the following correct limit formulas for planar, cylindrical, and spherical blast waves.

1) Planar blast wave ($\alpha = 0$):

$$\begin{aligned}\tau &= \int_0^\lambda \sqrt{\frac{4z}{1 + 4z}}\,dz = \frac{1}{4}[2\sqrt{\lambda(4\lambda + 1)} \\ &\quad + \ell n(\sqrt{4\lambda + 1} - 2\sqrt{\lambda})]\end{aligned} \tag{19}$$

2) Cylindrical blast wave ($\alpha = 1$):

$$\tau = \int_0^\lambda \sqrt{\frac{4z^2}{1 + 4z^2}}\,dz = \frac{1}{2}\left[(1 + 4\lambda^2)^{\frac{1}{2}} - 1\right] \tag{20}$$

3) Spherical blast wave ($\alpha = 2$):

$$\tau = \int_0^\lambda \sqrt{\frac{4z^3}{1 + 4z^3}}\,dz \tag{21}$$

Equation (21) can be solved by numerical integration.

In Fig. 1a, the correct limit approximation for a cylindrical wave ($\alpha = 1$) is compared with experimental data[5] as well as Sakurai's first-order and second-order approximations (for $\lambda = 1.4$). Experimental measurements on shock trajectories from an inverse pinch discharge[5] are in excellent agreement with Eq. (20) down to $M = 1.16$, which is referred to as M_c. Further investigations are necessary to find the values of M_c for the correct limit formulas of Eqs. (19) and (21), respectively. Moreover, the correct limit shock trajectories for planar, spherical, and cylindrical waves are shown in Fig. 1b.

In this study, shock waves are classified as strong shocks ($M > 3.3$), intermediate shocks ($M_c \le M \le 3.3$), and weak shocks ($1 < M < M_c$). It should be noted that Eqs. (19–21) deviate from the classical weak shock decay law[6] as the shock velocity approaches the acoustic limit. Jones et al.[7] have suggested an additional correct limit equation for overpressure across a cylindrical blast wave in the form

$$\Delta p/p_0 = \gamma[2(\gamma + 1)]^{-1}\left[(3/8)^{-\frac{3}{5}}\right]\left\{\left[1 + (8/3)^{\frac{8}{5}}\lambda^2\right]^{\frac{3}{8}} - 1\right\}^{-1} \tag{22}$$

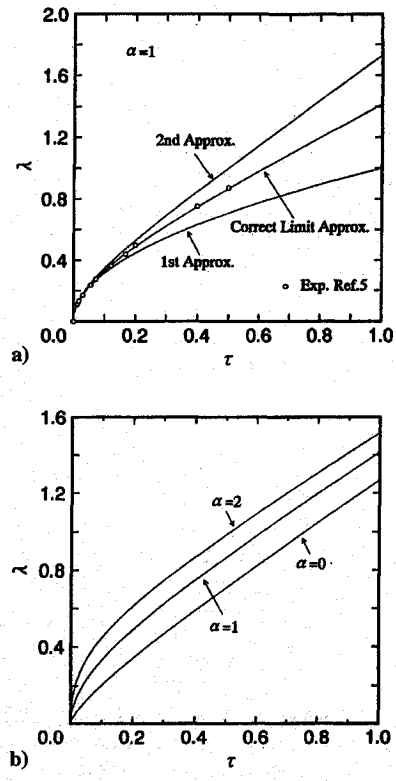

Fig. 1 Shock trajectories: a) comparison of correct limit approximation, experimental data,[5] and Sakurai's approximations for $\alpha = 1$ and $\gamma = 1.4$ and b) correct limit approximations for $\alpha = 0$, 1, and 2.

As $\lambda \to \infty$, the right-hand side approaches $\lambda^{-3/4}$, in agreement with weak shock decay law. Based on the Rankine–Hugoniot relation and Eq. (22), Jones et al. have obtained another trajectory equation that has been numerically integrated and compared with Eq. (20). As shown by Jones et al., the two trajectories differ by a maximum of less than 8% at $\lambda \sim 1.5$ ($M \sim 1.05$). However, the error decreases rapidly at lesser and greater distances.

Equations (19–21) are valid in the strong and intermediate shock regions and would deviate from the weak shock decay law only in the weak shock region. Therefore, they are still adequate as the first-order correct limit equations and are improvement upon Sakurai's second-order approximations.

Conclusions

A simplified approach has been proposed and applied to the development of cylindrical shock trajectory formula given by Vlases and Jones. Furthermore, the same technique has been used to develop the correct limit equations to predict the shock trajectories for planar and spherical blast waves. For intermediate and weak waves, the results achieved by the proposed method are improvement upon Sakurai's second-order approximations.

References

[1]Taylor, G. I., "The Formation of a Blast Wave by a Very Intense Explosion," *Proceedings of the Royal Society of London, Series A: Mathematical and Physical Sciences*, Vol. 201, March 1950, pp. 159–186.

[2]Sakurai, A., "On Propagation and Structure of the Blast Wave. I," *Journal of the Physical Society of Japan*, Vol. 8, No. 5, 1953, pp. 662–669.

[3]Lin, S. C., "Cylindrical Shock Waves Produced by Instantaneous Energy Release," *Journal of Applied Physics*, Vol. 25, No. 1, 1954, pp. 54–57.

[4]Sakurai, A., "On Propagation and Structure of the Blast Wave. II," *Journal of the Physical Society of Japan*, Vol. 9, No. 2, 1954, pp. 256–266.

[5]Vlases, G. C., and Jones, D. L., "Blast Waves from an Inverse Pinch Machine," *Physics of Fluids*, Vol. 9, No. 3, 1966, pp. 478–485.

[6]Whitham, G. B., *Linear and Nonlinear Waves*, Wiley, New York, 1974, Chap. 9.

[7]Jones, D. L., Goyer, G. G., and Plooster, M. N., "Shock Wave from a Lightning Discharge," *Journal of Geophysical Research*, Vol. 73, No. 10, 1968, pp. 3121–3127.

Observations of a Planar Jet Subjected to Large-Amplitude, Low-Frequency Disturbances

Robert B. Farrington* and Scott D. Claunch†
National Renewable Energy Laboratory, Golden, Colorado 80401

Introduction

THE behavior of jets under the influence of periodic disturbances has been of interest since the mid-1800s, including Plateau's[1] study of gravitationally induced liquid jets issuing from orifices vibrating from acoustical sources in contact with the vessel, and LeConte's[2] observation of the effect of acoustical tones from a musical trio on gas lights while at a dinner party. Brown[3] presented results on the effect of periodic forcing of a three-dimensional jet with Reynolds numbers of 1×10^2 to 2×10^2. The acoustic disturbances were introduced externally at frequencies ranging from 76 to 660 Hz. He observed both increased and suppressed growth of the jet.

A distinct saddle-back shape in the longitudinal velocity profile of a planar jet having nozzle aspect ratios of 20 and 25 and a Reynolds number of 1.3×10^4 was noticed by van der Hegge Zijnen[4] with the maxima near both ends of the profile being, at times, 10% greater than the centerline velocity. The saddle-back profile was accentuated by larger aspect ratios and by closing the ends to maintain two-dimensionality. Sato[5] used a channel approach (7.5–183.3 nozzle widths) to a nozzle with an aspect ratio varying from 10 to 91. He found that the disturbances changed velocity fluctuation levels along the jet centerline and that the Strouhal number equaled 0.23 for the symmetric fluctuations and 0.14 for the antisymmetric fluctuations.

Crow and Champagne[6] found that forced disturbances reduced the potential core of the jet and that the spread and axial velocity decays reached their asymptotic values more quickly than those of a natural jet. Browand and Laufer[7] introduced artificial disturbances and observed large-scale structures and the merging of vortex rings that they labeled pairing interactions. Zaman and Hussain,[8] who studied vortex pairing in air jets subjected to pure-tone acoustic disturbance, found both amplification and suppression of velocity fluctuations depending on the disturbance frequency.

Oster and Wygnanski[9] demonstrated that spreading rates can be significantly increased by disturbing the flow at frequencies at least an order of magnitude below the initial instability frequency. Ho and Huang[10] confirmed the effect of disturbing flows at frequencies lower than the natural instability frequency and noted that the spreading rate was sensitive to low disturbance frequencies and that collective interaction could result in 10 or more vortices coalescing.

The objective of this research is to determine the effect of large-amplitude, low-frequency disturbances on a free planar jet. Low-frequency, subaudible excitation is of interest in applications where higher excitation frequencies may be objectionable. The disturbance frequencies studied extended into the audible range, but the subaudible frequencies (below 20 Hz) are of particular interest.

Apparatus and Procedures

The nozzle, 2.54 cm wide and 119 cm long, was designed to approximate actual diffuser geometries used in building applications.[11] The axial distance was nondimensionalized by the nozzle width and

Received June 19, 1993; revision received Aug. 2, 1995; accepted for publication Aug. 9, 1995. This paper is declared a work of the U.S. Government and is not subject to copyright protection in the United States.

*Senior Mechanical Engineer, Building and Energy Systems Division, 1617 Cole Boulevard.

†Research Participant, Building and Energy Systems Division, 1617 Cole Boulevard.